ACS Medicinal Chemistry Letters

pubs.acs.org/acsmedchemlett Letter

Chiral Analogues of PFI-1 as BET Inhibitors and Their Functional Role in Myeloid Malignancies

Bianca Altenburg,[#] Marcus Frings,[#] Jan-Hendrik Schöbel,[#] Jonas Goßen, Kristina Pannen, Kim Vanderliek, Giulia Rossetti, Steffen Koschmieder, Nicolas Chatain,[▽] and Carsten Bolm*[,▽]

Cite This: https://dx.doi.org/10.1021/acsmedchemlett.9b00625 Read Online

ACCESS | Metrics & More | Article Recommendations | Supporting Information

ABSTRACT: Structural analogues of PFI-1 varying at the sulfur core were prepared, and their activities as BET inhibitors in myeloid cell lines and primary cells from patients with acute myeloid leukemia were studied. Docking calculations followed by molecular dynamics simulations revealed the binding mode of the newly prepared inhibitors, suggesting explanations for the observed high enantiospecificity of the inhibitory activity.

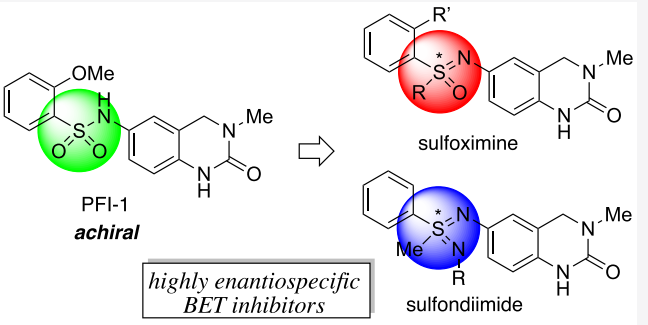

KEYWORDS: *BET inhibitors, acute myeloid leukemia (AML), sulfoximine, sulfondiimide, stereochemistry*

The bromodomain and extra-terminal (BET) motif protein BRD4 was first linked to cancer after the discovery of the BRD4−nuclear protein in testis (NUT) gene translocation resulting in NUT midline carcinoma, which is a very aggressive squamous cell carcinoma occurring primarily in adolescents.[1] Importantly, clinical responses were seen in selected patients using BET inhibitors that targeted BRD4.[2,3]

BET inhibitors are structurally diverse.[4−8] For example, **1** [(+)-JQ1][7] and **2** (OTX-015, MK8628, birabresib)[8] are triazolodiazepines that show potencies in the nanomolar range with pronounced selectivities in the BET family. Following work by Conway and co-workers[9] and Prinjha and co-workers,[10] Pfizer introduced 3,4-dihydro-3-methyl-2(1*H*)-quinazolinone **3** (PFI-1) as a BRD4-selective BET inhibitor.[11] The latter compound caught our attention because we hypothesized that its sulfonamidoyl group could be modified by (formal) atom exchange reactions leading to unprecedented sulfoximines **4** and sulfondiimides **5** (Chart 1).[12−14] In other systems, such sulfur core modifications had led to products with improved properties, including, for example, increased water solubility.[15] Furthermore, in contrast to **3**, compounds **4** and **5** are chiral, allowing studies of individual enantiomers.[16] Here we report on the preparation of these compounds and their characterization as new BET inhibitors in myeloid cell lines and primary cells from patients with acute myeloid leukemia (AML).

The syntheses of compounds **4** and **5** are summarized in Scheme 1. In general, they involved metal-catalyzed Buchwald/Hartwig- or Chan/Lam-type cross-coupling reactions of 3,4-dihydro-3-methyl-2(1*H*)-quinazolinones **8a** and **8b** with respective *N*H-sulfur derivatives (for details, see the Supporting Information). The latter were prepared by standard synthetic protocols leading to N-unfunctionalized sulfoximines **6**[17,18] and sulfondiimides **7**.[19] Enantiopure compounds **4** and **5a** were obtained by preparative CSP-HPLC (for **4c** and **7a**), resolution of diastereomeric salts (for **6a**), and asymmetric synthesis (for **6b**).

Since the initial description of the BRD4−NUT fusion, BRD4 has been examined in a variety of cancer types and found to be a potential therapeutic target in AML and myeloproliferative neoplasms.[20,21] AML is a heterogeneous disease characterized by a differentiation block and uncontrolled proliferation of hematopoietic stem and progenitor cells.[22] Approximately 97% of patients harbor clonal somatic abnormalities, including mutations in the FMS-like tyrosine kinase 3 (FLT3) of up to 38%.[23] Two main variations of mutations are described: the more frequent internal-tandem duplications (ITDs) and tyrosine kinase domain (TKD) mutations.[22] Recently, the FLT3 inhibitor midostaurin has been approved as targeted therapy in combination with chemotherapy for the treatment of FLT3-mutant AML on the basis of a phase 3 clinical trial.[24] However, additional

Special Issue: Medicinal Chemistry: From Targets to Therapies

Received: December 19, 2019
Accepted: April 2, 2020
Published: April 2, 2020

Chart 1. Known BET Inhibitors 1−3 and Newly Prepared Compounds 4 and 5

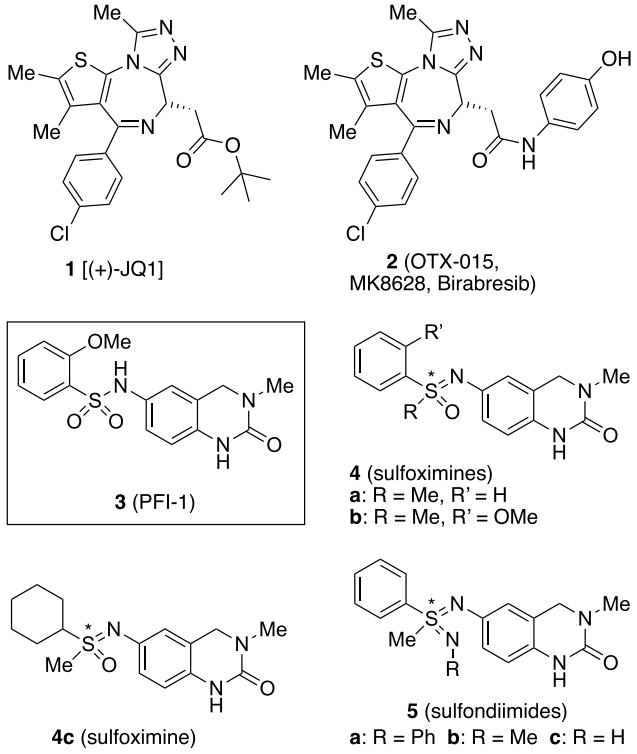

Scheme 1. Cross-Coupling Partners

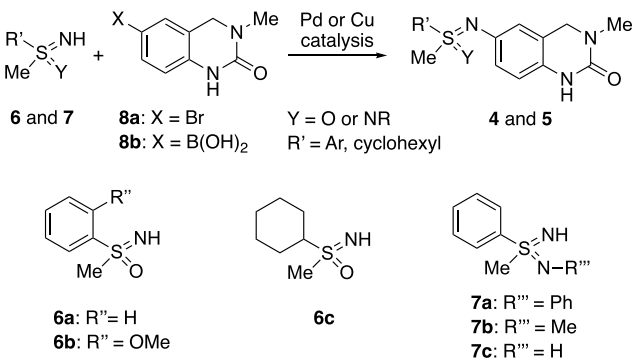

mutations increase the risk of therapy failure in FLT3-mutant and other subtypes of AML.

The BET motif family consists of four members in mammals: BRD2, BRD3, BRD4, and the testis-specific BRDT.[4−6] They share a conserved structure of two bromodomains (BRDs), an extraterminal recruitment (ET) domain, and some other motifs, like A, B, or SEED motifs. Furthermore, BRD4 and BRDT have a C-terminal motif (CTM).[5] While the ET domain takes part in protein−protein interactions, the C-terminal domain interacts with the positive transcription elongation factor b (p-TEFb).[5] The bromodomains contain around 110 amino acids and structurally form two loops (ZA and BC) and four α-helices (α_Z, α_A, α_B, and α_C).[25] The four α-helices build a hydrophobic pocket that recognizes acetylated lysines (K_{ac}) on proteins, such as histones.[26]

BRD4 and the other BET-BRDs can bind to acetylated lysine residues of N-terminal histone tails through their bromodomains and recruit the mediator and p-TEFb complex. Hence, BET-BRD proteins are termed epigenetic readers.[27] Hexamethylene bisacetamide-inducible protein 1 (HEXIM1) inhibits the p-TEFb complex through binding to 7SK small nuclear RNA. BRD4 displaces HEXIM1 from p-TEFb, which then becomes activated and subsequently phosphorylates the carboxy-terminal domain of RNA polymerase II to start transcription of BRD4-dependent genes.[27] Together, induction of HEXIM1 and reduction of MYC expression proved to be a potential biomarker in a clinical trial of BET.[28]

The activity of BRD4 in regulating and accelerating cell cycle progression through the regulation of gene expression in myeloid malignancies makes it a promising pharmaceutical target. Although BET inhibition is a matter of intensive ongoing research, recent clinical trials have encountered unexpected dose-limiting toxicity of BET inhibitors, including vomiting, headaches, and back pain,[28] as well as thrombocytopenia.[29] Thus, novel BET inhibitors that show optimized BET family member specificity are of interest to improve the tolerability in order to include long-term improvements of prognosis and quality of life in patients with AML and other myeloid malignancies. Optimization of dosing regimens and provision of treatment options in case of resistance emergence are conceivable.

Consequently, we decided to characterize the functional role of the aforementioned PFI-1 analogues in myeloid cell lines and primary cells from patients with AML. To analyze whether **4** and **5** had activity in cellular assays, MTT viability assays with HEL, Molm-14, and K562 cells, which are erythroleukemia, AML, and chronic myeloid leukemia (CML) (terminal blast phase) cell lines that are positive for JAK2 V617F-, FLT3-ITD-, and BCR-ABL, respectively, were performed. Initially, only racemates of the potential inhibitors were applied. This study showed that several compounds were active, and among them, sulfoximine **4b** and sulfondiimide **5a** were most efficient in reducing the relative metabolic activity of HEL and Molm-14 cells at a concentration of 10 μM (Figure S1). Sulfondiimides **5b** and **5c** showed lower efficacies. None of the compounds significantly affected the growth of the BET-inhibitor-insensitive cell line K562.

With the intention to take advantage of the stereochemistry at sulfur, the inhibitory activity of racemic **4a** on HEL, Molm-14, and K562 was compared to the effects induced by the individual enantiomers of **4a**. PFI-1 (**3**) was applied as a control. As envisaged, (*S*)-**4a** and (*R*)-**4a** behaved very differently. While treatment with 1 μM (*S*)-**4a** led to a significant decrease in relative metabolic activity of the HEL cells in comparison with 1 μM PFI-1 (37 ± 6% vs 73 ± 13%) (Figure 1A), no effect was observed with 1 μM (*R*)-**4a**, for which the result was comparable to the DMSO control (Figure 1A,B). Thus, the stereogenic center at sulfur significantly affected the efficacy of **4a**, with the *S* enantiomer being superior to both the racemic mixture of **4a** and the standard compound PFI-1. Similar effects were observed in the Molm14 cell line (55 ± 1% with 1 μM (*S*)-**4a** vs 80 ± 1% with 1 μM PFI-1) (Figure 1C). The IC_{50} values calculated in HEL and Molm-14 cells showed that (*S*)-**4a** was the most efficient compound, with concentrations of 0.5 μM (PFI-1: 2.0 μM) and 1.0 μM (PFI-1: 2.7 μM), respectively (Figure 1B,D). In contrast to HEL and Molm-14 cells, K562 cells remained mostly unaffected and never reached an IC_{50} (Figure 1E,F).

Applying single enantiomers of **4b** and **5a** in MTT assays revealed that also for **4b** the *S* enantiomer was superior over the *R*-configured compound (Figure S2). For **5a**, however, the

https://dx.doi.org/10.1021/acsmedchemlett.9b00625
ACS Med. Chem. Lett. XXXX, XXX, XXX−XXX

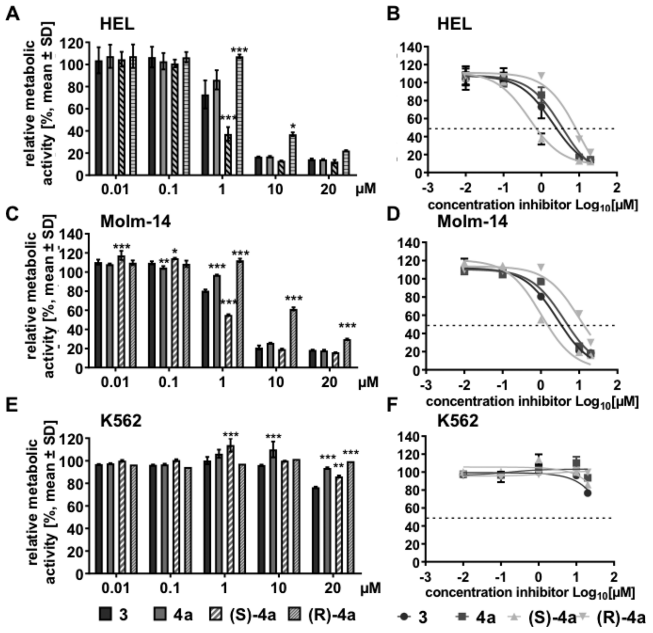

Figure 1. Marked differences in the efficacy of enantiomeric compounds. (A) HEL, (C) Molm-14 and (E) K562 cells were treated with PFI-1 (**3**), *rac*-**4a**, (*S*)-**4a**, and (*R*)-**4a** at concentrations of 10 nM, 100 nM, 1 μM, 10 μM, and 20 μM for 72 h. IC_{50} values calculated from MTT assays with (B) HEL, (D) Molm-14, and (E) K562 cells after compound treatment for 72 h. All data are normalized to the DMSO control and shown as mean ± SD. Graphs show combinations of three independent experiments. Statistics refer to **3**. **, $p < 0.01$; ***, $p < 0.001$.

absolute configuration had only a minor effect on the compound efficacy.

Next, we analyzed the selectivities of (*S*)-**4a** and PFI-1 for 76 bromodomain-containing proteins in a thermal shift assay (TSA) (BromoMELT assay, Reaction Biology Corp., Malvern, PA, USA). The TSA demonstrated a slightly higher selectivity of (*S*)-**4a** versus PFI-1 for BRD2/4 (ΔT_m of 5 vs 4 °C for BRD4 and 3.5 vs 2.5 °C for BRD2-1) (Figure 2A,B; see the Supporting Information for the full data sets for PFI-1 and (*S*)-4a). At the same time, the ΔT_m is reduced for BRDT-2 and slightly for BRD3 [(*S*)-**4a** vs PFI-1]. Therefore, we confirmed the binding of (*S*)-**4a** to BET proteins and demonstrated a better selectivity profile of (*S*)-**4a** for BRD2 and BRD4 in comparison with PFI-1.

Several studies confirmed induction of growth arrest and apoptosis using the BET inhibitors JQ1 (**1**) and OTX015 (**2**).[8,20,30] Therefore, we evaluated whether (*S*)-**4a** and further compounds led to reduced proliferation and disturbed cell cycle progression. Indeed, proliferation of HEL and Molm-14 cells was significantly reduced by (*S*)-**4a** compared with PFI-1 (Figures 2C and S3A−C), whereas the number of K562 cells was only slightly affected by (*S*)-**4a** treatment, in line with data on another BET inhibitor.[31]

Analysis of the cell cycle progression confirmed that PFI-1 and (*S*)-**4a** led to an increase in the G0/G1 phase, a decrease in the S phase, and in some cases an increase in the sub-G1 phase (Figures S3D and S2E). Again, (*S*)-**4a** was more effective than PFI-1 in perturbing the transition from the G1 phase to the S phase, and an increase in the sub-G1 peak was observed.

Next, the direct effects of the novel compounds on viability and apoptosis were determined. In HEL and Molm-14 cells, 55

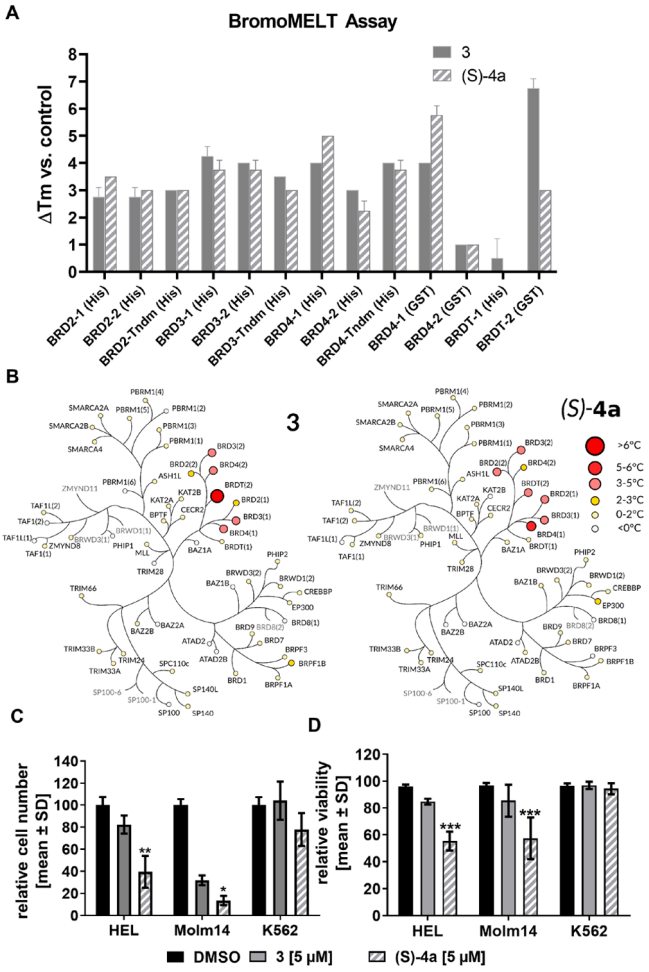

Figure 2. Higher selectivity and potency of (*S*)-**4a**. (A) Thermal shift assay (TSA) (BromoMELT assay) of PFI-1 (**3**) and (*S*)-**4a** in duplicate at 10 μM. Shown are the values of ΔT_m vs control for the BET domain protein family. Full analyses for PFI-1 and (*S*)-4a are provided in the Supporting Information. (B) TSA data for PFI-1 (**3**) and (*S*)-**4a**. Temperature shifts are indicated by reddish circles with increasing radii for higher T_m values as indicated.[32] (C) HEL, Molm-14 and K562 cells were treated with either DMSO or 5 μM of compounds or (*S*)-**4a**. Comparison of cell proliferation after 72 h of treatment. Three independent experiments combined. All data displayed as mean ± SD. Statistics: 5 μM of PFI-1 compared to 5 μM of (*S*)-**4a**. (D) Bar graph illustrating significant viability loss by 5 μM (*S*)-**4a** treatment of HEL and Molm-14 cells after 72 h of treatment. All data are shown as mean ± SD. Statistics: **3** compared to (*S*)-**4a**. *$p < 0.05$, **$p < 0.01$, ***$p < 0.001$.

μM PFI-1 reduced the cell viability to 85 ± 2% or 85 ± 12%, respectively, while 5 μM (*S*)-**4a** diminished it to 55 ± 7% or 57 ± 16%, respectively, after 72 h of treatment (Figures 2D and S4A,B). PARP1 cleavage, as a marker of apoptosis, was confirmed in (*S*)-**4a**-treated HEL cells and more pronounced in Molm-14 cells (Figure S4D). In the DMSO control, PARP1 cleavage was partly detected, mostly as a result of massive proliferation of cells without BRD4 inhibitor and therefore a lack of nutrients (Figure S4D),[33] which was also supported by the higher amount of uncleaved PARP1 protein (upper band) in DMSO- and (*R*)-**4a**-treated cells (Figure S4D; prominent in Molm14 cells). As expected, no reduction of viability and PARP1 cleavage was observed in K562 cells (Figure S4C,D).

Taken together, the results show that (*S*)-**4a** was more efficient in reducing the viability of Molm-14 and HEL cells

https://dx.doi.org/10.1021/acsmedchemlett.9b00625
ACS Med. Chem. Lett. XXXX, XXX, XXX−XXX

than PFI-1. The major effect of BRD4 inhibition was to block proliferation and cell cycle progression.

BET protein inhibition is correlated with decreased expression of Aurora kinase B (AURKB) and increased expression of HEXIM1, and HEXIM1 participates in the subsequent growth arrest of AML cell lines.[34,35] Therefore, we performed Western blot analysis and observed that HEXIM1 protein was increased in HEL and Molm-14 cells after 24 h of treatment with 5 μM PFI-1 and even more after treatment with (*S*)-**4a** (Figure 3A,B). In contrast, (*R*)-**4a** treatment did not

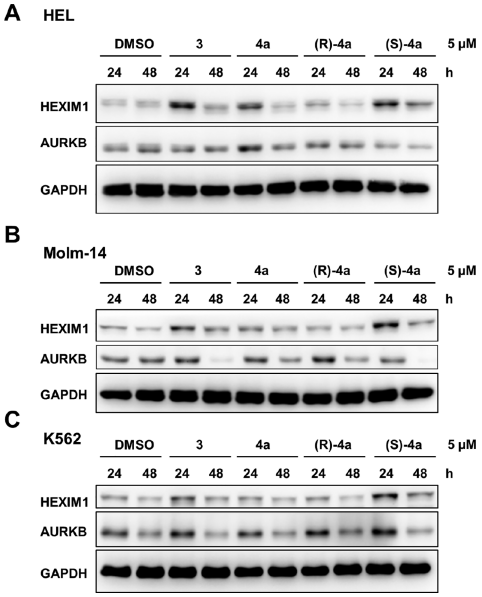

Figure 3. Western Blot analysis of HEXIM1 protein in compound-treated HEL, Molm14, and K562 cells. (A) HEL, (B) Molm14, and (C) K562 cells were incubated with DMSO or the indicated compounds at 5 μM for 24 or 48 h. Specific antibodies detecting HEXIM1, Aurora kinase B (AURKB), and GAPDH were used. GAPDH served as a loading control.

increase the HEXIM1 protein level. Surprisingly, (*R*)-**4a** reduced AURKB in Molm-14 cells and K562 cells after 48 h, but at least the result in K562 cells was DMSO-dependent. Nevertheless, (*S*)-**4a** most efficiently reduced AURKB protein levels in HEL and Molm-14 cells (Figure 3).

Although HEXIM1 protein was upregulated in K562 cells treated with PFI-1 and (*S*)-**4a** (Figure 3C), cell viability was not reduced by BRD4 inhibition (Figures 1 and 2). Hence, HEXIM1 alone cannot ablate CML cell line proliferation and viability. Interestingly, HEXIM1 protein decreased already 48 h after treatment, demonstrating a relatively short half-life of the used BRD4 inhibitors and probably explaining relatively low induction of apoptosis. On the other hand, AURKB protein behaved in the opposite way, most likely demonstrating the protein half-life before its proteasomal degradation. Preincubation of PFI-1 and (*S*)-**4a** in medium and subsequent treatment of HEL, K562, and Molm-14 cells demonstrated compound stability and robust induction of HEXIM1, especially by (*S*)-**4a** (Figure S5).

To support our cell line data, AML patient peripheral blood mononuclear cells (PBMCs), carrying FLT3-ITD or tyrosine kinase domain (FLT3-TKD) mutations were isolated and applied into colony formation (CFU) assays. Healthy-donor PBMCs or CD34+ cells were used to analyze general cytotoxicity.

Clonogenic growth of healthy donor cells (PBMCs and CD34+) was reduced in both 1 μM and 5 μM compound treatments (Figure 4A), as demonstrated already for PFI-1 and

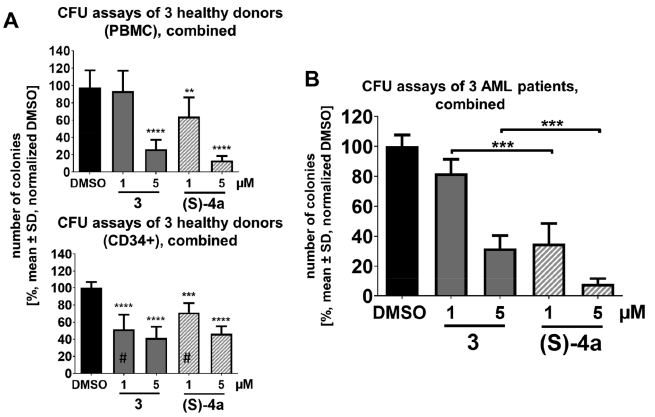

Figure 4. (*S*)-**4a** reduces clonogenic growth of primary AML patient cells more efficiently than PFI-1. (A) CFU assays with (top) healthy-donor peripheral blood mononuclear cells (PBMCs) or (bottom) CD34+ cells (# indicates only two treatments at 1 μM). (B) CFU assays with bone marrow monocuclear cells (BMMCs) of three FLT3-ITD- or -TKD-mutated AML patient samples combined and normalized to the DMSO control. Experiments were performed in triplicate. All of the data are shown as mean ± SD. **, $p < 0.01$; ***, $p < 0.001$.

OTX015.[31,36] Importantly, (*S*)-**4a** at 1 and 5 μM reduced the colony number of bone marrow mononuclear cells (BMMCs) isolated from AML patients more efficiently than the standard compound PFI-1 (Figure 4B). More HD and AML samples need to be analyzed in the future.

With the goal to gain a more fundamental understanding of the binding mode of the newly prepared inhibitors and to develop a comprehension for the enantiospecific inhibitory activity, in silico models of the structural determinants of BRD4−ligand complexes were obtained by performing docking calculations followed by molecular dynamics (MD) simulations. For this purpose, the X-ray structure of the first bromodomain of human BRD4 in complex with the inhibitor PFI-1 (PDB ID 4E96) was used. The best-performing ligand according to the Glide XP scoring function (see the Supporting Information for details) is (*S*)-**4a**, while (*R*)-**4a** is the worst (see Table S8).

In their best binding poses (see Methods in the Supporting Information for details), the anchoring hydrogen-bonding interactions with ASN140 and the water-mediated interaction with TYR97 of BRD4, observed in the X-ray complex of PFI-1 (Figure 5E), are preserved for both (*S*)-**4a** (Figures 5A,B) and (*R*)-**4a** (Figure 5C,D). However, (*S*)-**4a** orients the anchoring 3,4-dihydro-3-methyl-2(1*H*)-quinazolinone core toward the BC loop, and the sulfoximidoyl group points toward the hydrophobic patch consisting of ILE146, PRO82, and TRP81 (Figure 5A,B).[37] Differently, in (*R*)-**4a** the latter substituent points toward the opposite direction, suggesting the loss of the hydrophobic-patch interactions and the exposure of the apolar phenyl moiety to the solvent (Figures 5C,D). Therefore, we expect (*R*)-**4a** to be a weaker binder with respect both (*S*)-**4a** and PFI-1.

https://dx.doi.org/10.1021/acsmedchemlett.9b00625
ACS Med. Chem. Lett. XXXX, XXX, XXX−XXX

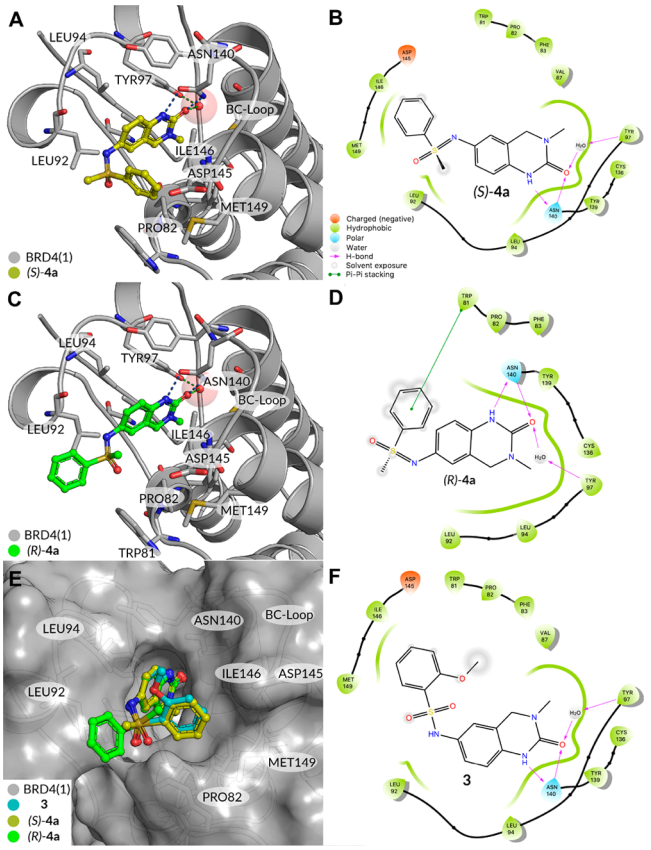

Figure 5. (A–D) Best binding poses of (A) (*S*)-**4a** and (C) (*R*)-**4a** in three dimensions and (B, D) the corresponding two-dimensional (2D) representations of nonbonded interactions. In (A) and (C), hydrogen bonds are shown in blue, water-mediated hydrogen bonds are denoted as green dashed lines, and the position of water 380 is shown as a red sphere. The phenyl moiety of (*S*)-**4a** shows a distinct kink toward ILE146 (dihedral angle φ(CNSC) = 56.6°). The *R* enantiomer does not show this kink (φ(CNSC) = 175.5°). In (B) and (D), hydrogen bonding is denoted by the magenta arrows. The hydrophobic surface area is shown as a green line, and the color coding of the pocket residues is explained in the legend of (B). (E) Direct comparison of the crystal pose orientation of PFI-1 (**3**) and the best binding poses of (*S*)-**4a** and (*R*)-**4a**, with the van der Waals surface of BRD4 shown as a gray surface. (F) 2D representation of the binding conformation of **3** in the crystal structure (PDB ID 4E96). The same color code as in (B) and (D) was implemented.

Interestingly, (*S*)-**4a** performed better than PFI-1 in our in silico experiments. A significant difference between (*S*)-**4a** and PFI-1 is the hybridization state of the nitrogen atom on passing from sulfonamide to sulfoximine (sp^3 to sp^2, respectively). Increasing the s character of the nitrogen lone pair decreases the hydrogen-bond acceptor strength ($sp^3 > sp^2 > sp$).[38] The sp^3-hybridized nitrogen in PFI-1 is therefore a stronger hydrogen-bond acceptor than the sp^2-hybridized nitrogen in (*S*)-**4a**, suggesting slightly better solvation and higher hydrophilicity. Therefore, the slightly more hydrophobic (*S*)-**4a** would be better stabilized than PFI-1 in the hydrophobic binding pocket of BRD4. Also, the sp^2-hybridized nitrogen in the sulfoximine moiety reduces the flexibility of (*S*)-**4a**, since the free rotation around the N–S bond (dihedral angle φ(–CNSC)) is lost. As a result, (*S*)-**4a** is restricted in its orientation. The restriction of a small molecule's motion on binding to a protein usually causes a loss of configurational entropy and thus a penalty in binding affinity.[39,40] The single orientation of the N–S bond in (*S*)-**4a** causes a lower loss of entropy with respect to PFI-1 upon binding. These observations together point to (*S*)-**4a** having a higher binding affinity toward BRD4 compared with PFI-1.

In summary, we found a new BET inhibitor with activity in myeloid cell lines and primary cells from patients with acute myeloid leukemia (AML). The most effective compound, **4a**, has a stereogenic center at sulfur, and its absolute configuration dictates its efficacy. The data show that (*S*)-**4a** is superior to well-studied PFI-1. The *R* enantiomer of **4a** is essentially inactive.

Although the BET inhibitors, including PFI-1 and our newly prepared (*S*)-**4a**, showed some degree of activity on healthy control cells, the effects on AML cells were more pronounced. Therapy with BET protein bromodomain antagonists is of high interest and may be beneficial for particular patients. In addition, combination therapy of BRD4 inhibitors with specific tyrosine kinase inhibitors should be further evaluated. Thus, subsequent research is needed to investigate whether (*S*)-**4a** can be used as a single therapeutic agent or in combination therapy for AML.

■ ASSOCIATED CONTENT

Supporting Information

The Supporting Information is available free of charge at https://pubs.acs.org/doi/10.1021/acsmedchemlett.9b00625.

BromoMELT assay for PFI-1 (PDF)

BromoMELT assay for (*S*)-**4a** (PDF)

Chemical syntheses, NMR spectra, HPLC traces, biological testings, and computational studies (PDF)

■ AUTHOR INFORMATION

Corresponding Author

Carsten Bolm – *Institute of Organic Chemistry, RWTH Aachen University, 52074 Aachen, Germany;* orcid.org/0000-0001-9415-9917; Email: Carsten.Bolm@oc.rwth-aachen.de

Authors

Bianca Altenburg – *Department of Hematology, Oncology, Hemostaseology, and Stem Cell Transplantation, Faculty of Medicine, RWTH Aachen University, 52074 Aachen, Germany*

Marcus Frings – *Institute of Organic Chemistry, RWTH Aachen University, 52074 Aachen, Germany;* orcid.org/0000-0002-6228-1229

Jan-Hendrik Schöbel – *Institute of Organic Chemistry, RWTH Aachen University, 52074 Aachen, Germany*

Jonas Goßen – *Institute of Neuroscience and Medicine (INM-9)/Institute for Advanced Simulation (IAS-5), Forschungszentrum Jülich, 52425 Jülich, Germany; Faculty of Mathematics, Computer Science and Natural Sciences, RWTH Aachen University, 52074 Aachen, Germany*

Kristina Pannen – *Department of Hematology, Oncology, Hemostaseology, and Stem Cell Transplantation, Faculty of Medicine, RWTH Aachen University, 52074 Aachen, Germany*

Kim Vanderliek – *Department of Hematology, Oncology, Hemostaseology, and Stem Cell Transplantation, Faculty of Medicine, RWTH Aachen University, 52074 Aachen, Germany*

Giulia Rossetti – *Department of Hematology, Oncology, Hemostaseology, and Stem Cell Transplantation, Faculty of Medicine, RWTH Aachen University, 52074 Aachen, Germany; Institute of Neuroscience and Medicine (INM-9)/Institute for Advanced Simulation (IAS-5) and Jülich Supercomputing*

https://dx.doi.org/10.1021/acsmedchemlett.9b00625
ACS Med. Chem. Lett. XXXX, XXX, XXX–XXX

Centre (JSC), Forschungszentrum Jülich, 52425 Jülich, Germany; orcid.org/0000-0002-2032-4630

Steffen Koschmieder − *Department of Hematology, Oncology, Hemostaseology, and Stem Cell Transplantation, Faculty of Medicine, RWTH Aachen University, 52074 Aachen, Germany*

Nicolas Chatain − *Department of Hematology, Oncology, Hemostaseology, and Stem Cell Transplantation, Faculty of Medicine, RWTH Aachen University, 52074 Aachen, Germany*

Complete contact information is available at: https://pubs.acs.org/10.1021/acsmedchemlett.9b00625

Author Contributions

[#]B.A., M.F., and J.-H.S. contributed equally (shared first authorship). The manuscript was written through contributions of all authors. All of the authors approved the final version of the manuscript.

Author Contributions

[▽]N.C. and C.B. have shared last authorship.

Funding

This work was supported by RWTH Aachen University through Seed Funds Project OPSF496.

Notes

The authors declare no competing financial interest.

Part of this work was generated within the medical thesis work of B.A., and part of this work was generated within the Master's thesis of K.V. A patent application was submitted.

■ ACKNOWLEDGMENTS

We are grateful to Cornelia Vermeeren (RWTH Aachen University) for the preparative CSP-HPLC separation of two compounds. The support of Susanne Grünebaum (RWTH Aachen University) in compound syntheses is highly appreciated.

■ ABBREVIATIONS

AML, acute myeloid leukemia; BET, bromodomain and extra-terminal; BMMC, bone marrow mononuclear cell; CML, chronic myeloid leukemia; CSP, chiral stationary phase; CTM, C-terminal motif; FLT3, FMS-like tyrosine kinase 3; GAPDH, glyceraldehyde-3-phosphatedehydrogenase; HEL, human erythroleukemia cell line; HEXIM1, hexamethylene bisacetamide-inducible protein 1; HPLC, high-performance liquid chromatography; MCAP, mitotic chromosome associated protein; NUT, nuclear protein in testis; PMF, primary myelofibrosis; PBMC, peripheral blood mononuclear cell; PV, polycythemeia vera; p-TEFb, positive transcription elongation factor b; SD, standard deviation; TKD, tyrosine kinase domain

■ REFERENCES

(1) French, C. A.; Miyoshi, I.; Kubonishi, I.; Grier, H. E.; Perez-Atayde, A. R.; Fletcher, J. A. BRD4−NUT fusion oncogene: a novel mechanism in aggressive carcinoma. *Cancer Res.* **2003**, *63*, 304−307.

(2) Stathis, A.; Zucca, E.; Bekradda, M.; Gomez-Roca, C.; Delord, J.-P.; de La Motte Rouge, T.; Uro-Coste, E.; de Braud, F.; Pelosi, G.; French, C. A. Clinical response of carcinomas harboring the BRD4−NUT oncoprotein to the targeted bromodomain inhibitor OTX015/MK-9628. *Cancer Discovery* **2016**, *6*, 492−500.

(3) Liu, Z.; Wang, P.; Chen, H.; Wold, E. A.; Tian, B.; Brasier, A. R.; Zhou, J. Drug discovery targeting bromodomain-containing protein 4. *J. Med. Chem.* **2017**, *60*, 4533−4558.

(4) Wu, Q.; Heidenreich, D.; Zhou, S.; Ackloo, S.; Krämer, A.; Nakka, K.; Lima-Fernandes, E.; Deblois, G.; Duan, S.; Vellanki, R. N.; Li, F.; Vedadi, M.; Dilworth, J.; Lupien, M.; Brennan, P. E.; Arrowsmith, C. H.; Müller, S.; Fedorov, O.; Filippakopoulos, P.; Knapp, S. A chemical toolbox for the study of bromodomains and epigenetic signaling. *Nat. Commun.* **2019**, *10*, 1915.

(5) Jung, M.; Gelato, K. A.; Fernández-Montalván, A.; Siegel, S.; Haendler, B. Targeting BET bromodomains for cancer treatment. *Epigenomics* **2015**, *7*, 487−501.

(6) Filippakopoulos, P.; Knapp, S. Targeting bromodomains: epigenetic readers of lysine acetylation. *Nat. Rev. Drug Discovery* **2014**, *13*, 337−356.

(7) Filippakopoulos, P.; Qi, J.; Picaud, S.; Shen, Y.; Smith, W. B.; Fedorov, O.; Morse, E. M.; Keates, T.; Hickman, T. T.; Felletar, I.; Philpott, M.; Munro, S.; McKeown, M. R.; Wang, Y.; Christie, A. L.; West, N.; Cameron, M. J.; Schwartz, B.; Heightman, T. D.; La Thangue, N.; French, C. A.; Wiest, O.; Kung, A. L.; Knapp, S.; Bradner, J. E. Selective inhibition of BET bromodomains. *Nature* **2010**, *468*, 1067−1073.

(8) Coude, M. M.; Braun, T.; Berrou, J.; Dupont, M.; Bertrand, S.; Masse, A.; Raffoux, E.; Itzykson, R.; Delord, M.; Riveiro, M. E.; Herait, P.; Baruchel, A.; Dombret, H.; Gardin, C. BET inhibitor OTX015 targets BRD2 and BRD4 and decreases c-MYC in acute leukemia cells. *Oncotarget* **2015**, *6*, 17698−17712.

(9) Hewings, D. S.; Wang, M.; Philpott, M.; Fedorov, O.; Uttarkar, S.; Filippakopoulos, P.; Picaud, S.; Vuppusetty, C.; Marsden, B.; Knapp, S.; Conway, S. J.; Heightman, T. D. 3,5-Dimethylisoxazoles act as acetyl-lysine-mimetic bromodomain ligands. *J. Med. Chem.* **2011**, *54*, 6761−6770.

(10) Dawson, M. A.; Prinjha, R. K.; Dittmann, A.; Giotopoulos, G.; Bantscheff, M.; Chan, W.-I.; Robson, S. C.; Chung, C.-w.; Hopf, C.; Savitski, M. M.; Huthmacher, C.; Gudgin, E.; Lugo, D.; Beinke, S.; Chapman, T. D.; Roberts, E. J.; Soden, P. E.; Auger, K. R.; Mirguet, O.; Doehner, K.; Delwel, R.; Burnett, A. K.; Jeffrey, P.; Drewes, G.; Lee, K.; Huntly, B. J. P.; Kouzarides, T. Inhibition of BET recruitment to chromatin as an effective treatment for MLL-fusion leukaemia. *Nature* **2011**, *478*, 529−533.

(11) Fish, P. V.; Filippakopoulos, P.; Bish, G.; Brennan, P. E.; Bunnage, M. E.; Cook, A. S.; Federov, O.; Gerstenberger, B. S.; Jones, H.; Knapp, S.; Marsden, M. J.; Nocka, K.; Owen, D. R.; Philpott, M.; Picaud, S.; Primiano, M. J.; Ralph, M. J.; Sciammetta, N.; Trzupek, J. D. Identification of a chemical probe for bromo and extra C-terminal bromodomain inhibition through optimization of a fragment-derived hit. *J. Med. Chem.* **2012**, *55*, 9831−9837.

(12) Lücking, U. Neglected sulfur(VI) pharmacophores in drug discovery: exploration of novel chemical space by the interplay of drug design and method development. *Org. Chem. Front.* **2019**, *6*, 1319−1324.

(13) Lücking, U. Sulfoximines: a neglected opportunity in medicinal chemistry. *Angew. Chem., Int. Ed.* **2013**, *52*, 9399−9408.

(14) Frings, M.; Bolm, C.; Blum, A.; Gnamm, A. Sulfoximines from a medicinal chemist's perspective: physicochemical and in vitro parameters relevant for drug discovery. *Eur. J. Med. Chem.* **2017**, *126*, 225−245.

(15) Foote, K. M.; Nissink, J. W. M.; McGuire, T.; Turner, P.; Guichard, S.; Yates, J. W. T.; Lau, A.; Blades, K.; Heathcote, D.; Odedra, R.; Wilkinson, G.; Wilson, Z.; Wood, C. M.; Jewsbury, P. J. Discovery and characterization of AZD6738, a potent inhibitor of ataxia telangiectasia mutated and Rad3 related (ATR) kinase with application as an anticancer agent. *J. Med. Chem.* **2018**, *61*, 9889−9907.

(16) Park, S. J.; Baars, H.; Mersmann, S.; Buschmann, H.; Baron, J. M.; Amann, P. M.; Czaja, K.; Hollert, H.; Bluhm, K.; Redelstein, R.; Bolm, C. N-Cyano sulfoximines: COX inhibition, anticancer activity, cellular toxicity, and mutagenicity. *ChemMedChem* **2013**, *8*, 217−220.

(17) Bull, J. A.; Degennaro, L.; Luisi, R. Straightforward strategies for the preparation of NH-sulfoximines: a serendipitous story. *Synlett* **2017**, *28*, 2525−2538.

(18) Bizet, V.; Hendriks, C. M. M.; Bolm, C. Sulfur imidations: access to sulfimides and sulfoximines. *Chem. Soc. Rev.* **2015**, *44*, 3378−3390.

(19) Candy, M.; Guyon, C.; Mersmann, S.; Chen, J.-R.; Bolm, C. Synthesis of sulfondiimines by N-chlorosuccinimide-mediated oxidative imination of sulfiliminium salts. *Angew. Chem., Int. Ed.* **2012**, *51*, 4440−4443.
(20) Zuber, J.; Shi, J.; Wang, E.; Rappaport, A. R.; Herrmann, H.; Sison, E. A.; Magoon, D.; Qi, J.; Blatt, K.; Wunderlich, M.; Taylor, M. J.; Johns, C.; Chicas, A.; Mulloy, J. C.; Kogan, S. C.; Brown, P.; Valent, P.; Bradner, J. E.; Lowe, S. W.; Vakoc, C. R. RNAi screen identifies Brd4 as a therapeutic target in acute myeloid leukaemia. *Nature* **2011**, *478*, 524−528.
(21) Kleppe, M.; Koche, R.; Zou, L.; van Galen, P.; Hill, C. E.; Dong, L.; De Groote, S.; Papalexi, E.; Hanasoge Somasundara, A. V.; Cordner, K.; Keller, M.; Farnoud, N.; Medina, J.; McGovern, E.; Reyes, J.; Roberts, J.; Witkin, M.; Rapaport, F.; Teruya-Feldstein, J.; Qi, J.; Rampal, R.; Bernstein, B. E.; Bradner, J. E.; Levine, R. L. Dual targeting of oncogenic activation and inflammatory signaling increases therapeutic efficacy in myeloproliferative neoplasms. *Cancer Cell* **2018**, *33*, 29−43.
(22) Kindler, T.; Lipka, D. B.; Fischer, T. FLT3 as a therapeutic target in AML: still challenging after all these years. *Blood* **2010**, *116*, 5089−5102.
(23) Coombs, C. C.; Tallman, M. S.; Levine, R. L. Molecular therapy for acute myeloid leukaemia. *Nat. Rev. Clin. Oncol.* **2016**, *13*, 305−318.
(24) Stone, R. M.; Mandrekar, S. J.; Sanford, B. L.; Laumann, K.; Geyer, S.; Bloomfield, C. D.; Thiede, C.; Prior, T. W.; Döhner, K.; Marcucci, G.; Lo-Coco, F.; Klisovic, R. B.; Wei, A.; Sierra, J.; Sanz, M. A.; Brandwein, J. M.; de Witte, T.; Niederwieser, D.; Appelbaum, F. R.; Medeiros, B. C.; Tallman, M. S.; Krauter, J.; Schlenk, R. F.; Ganser, A.; Serve, H.; Ehninger, G.; Amadori, S.; Larson, R. A.; Döhner, H. Midostaurin plus chemotherapy for acute myeloid leukemia with a FLT3 mutation. *N. Engl. J. Med.* **2017**, *377*, 454−464.
(25) Taniguchi, Y. The bromodomain and extra-terminal domain (BET) family: functional anatomy of BET paralogous proteins. *Int. J. Mol. Sci.* **2016**, *17*, 1849.
(26) Filippakopoulos, P.; Picaud, S.; Mangos, M.; Keates, T.; Lambert, J.-P.; Barsyte-Lovejoy, D.; Felletar, I.; Volkmer, R.; Müller, S.; Pawson, T.; Gingras, A.-C.; Arrowsmith, C. H.; Knapp, S. Histone recognition and large-scale structural analysis of the human bromodomain family. *Cell* **2012**, *149*, 214−231.
(27) Yang, Z.; Yik, J. H.; Chen, R.; He, N.; Jang, M. K.; Ozato, K.; Zhou, Q. Recruitment of P-TEFb for stimulation of transcriptional elongation by the bromodomain protein Brd4. *Mol. Cell* **2005**, *19*, 535−545.
(28) Postel-Vinay, S.; Herbschleb, K.; Massard, C.; Woodcock, V.; Soria, J.-C.; Walter, A. O.; Ewerton, F.; Poelman, M.; Benson, N.; Ocker, M.; Wilkinson, G.; Middleton, M. First-in-human phase I study of the bromodomain and extraterminal motif inhibitor BAY 1238097: emerging pharmacokinetic/pharmacodynamic relationship and early termination due to unexpected toxicity. *Eur. J. Cancer* **2019**, *109*, 103−110.
(29) Amorim, S.; Stathis, A.; Gleeson, M.; Iyengar, S.; Magarotto, V.; Leleu, X.; Morschhauser, F.; Karlin, L.; Broussais, F.; Rezai, K.; Herait, P.; Kahatt, C.; Lokiec, F.; Salles, G.; Facon, T.; Palumbo, A.; Cunningham, D.; Zucca, E.; Thieblemont, C. Bromodomain inhibitor OTX015 in patients with lymphoma or multiple myeloma: a dose-escalation, open-lable, pharmacokinetic, phase 1 study. *Lancet Haematol.* **2016**, *3*, e196−e204.
(30) Fiskus, W.; Sharma, S.; Qi, J.; Shah, B.; Devaraj, S. G. T.; Leveque, C.; Portier, B. P.; Iyer, S.; Bradner, J. E.; Bhalla, K. N. BET protein antagonist JQ1 is synergistically lethal with FLT3 tyrosine kinase inhibitor (TKI) and overcomes resistance to FLT3-TKI in AML cells expressing FLT-ITD. *Mol. Cancer Ther.* **2014**, *13*, 2315−2327.
(31) Picaud, S.; Da Costa, D.; Thanasopoulou, A.; Filippakopoulos, P.; Fish, P. V.; Philpott, M.; Fedorov, O.; Brennan, P.; Bunnage, M. E.; Owen, D. R.; Bradner, J. E.; Taniere, P.; O'Sullivan, B.; Muller, S.; Schwaller, J.; Stankovic, T.; Knapp, S. PFI-1, a highly selective protein interaction inhibitor, targeting BET Bromodomains. *Cancer Res.* **2013**, *73*, 3336−3346.
(32) Adopted from Reaction Biology Corp.: http://www.reactionbiology.com/webapps/site/BromoMelt.aspx.
(33) Krampe, B.; Al-Rubeai, M. Cell death in mammalian cell culture: molecular mechanisms and cell line engineering strategies. *Cytotechnology* **2010**, *62*, 175−188.
(34) Devaraj, S. G.; Fiskus, W.; Shah, B.; Qi, J.; Sun, B.; Iyer, S. P.; Sharma, S.; Bradner, J. E.; Bhalla, K. N. HEXIM1 induction is mechanistically involved in mediating anti-AML activity of BET protein bromodomain antagonist. *Leukemia* **2016**, *30*, 504−508.
(35) Sahni, J. M.; Gayle, S. S.; Bonk, K. L. W.; Vite, L. C.; Yori, J. L.; Webb, B.; Ramos, E. K.; Seachrist, D. D.; Landis, M. D.; Chang, J. C.; Bradner, J. E.; Keri, R. A. Bromodomain and extraterminal protein inhibition blocks growth of triple-negative breast cancers through the suppression of aurora kinases. *J. Biol. Chem.* **2016**, *291*, 23756−23768.
(36) Saenz, D. T.; Fiskus, W.; Qian, Y.; Manshouri, T.; Rajapakshe, K.; Raina, K.; Coleman, K. G.; Crew, A. P.; Shen, A.; Mill, C. P.; Sun, B.; Qiu, P.; Kadia, T. M.; Pemmaraju, N.; DiNardo, C.; Kim, M. S.; Nowak, A. J.; Coarfa, C.; Crews, C. M.; Verstovsek, S.; Bhalla, K. N. Novel BET protein proteolysis-targeting chimera exerts superior lethal activity than bromodomain inhibitor (BETi) against post-myeloproliferative neoplasm secondary (s) AML cells. *Leukemia* **2017**, *31*, 1951−1961.
(37) Vidler, L. R.; Brown, N.; Knapp, S.; Hoelder, S. Druggability analysis and structural classification of bromodomain acetyl-lysine binding sites. *J. Med. Chem.* **2012**, *55*, 7346−7359.
(38) Møller, K. H.; Kjaersgaard, A.; Hansen, A. S.; Du, L.; Kjaergaard, H. G. Hybridization of nitrogen determines hydrogen-bond acceptor strength: gas-phase comparison of redshifts and equilibrium constants. *J. Phys. Chem. A* **2018**, *122*, 3899−3908.
(39) Klebe, G.; Böhm, H. J. Energetic and entropic factors determining binding affinity in protein-ligand complexes. *J. Recept. Signal Transduction Res.* **1997**, *17*, 459−473.
(40) Chang, C. A.; Chen, W.; Gilson, M. K. Ligand configurational entropy and protein binding. *Proc. Natl. Acad. Sci. U. S. A.* **2007**, *104*, 1534−1539.

https://dx.doi.org/10.1021/acsmedchemlett.9b00625
ACS Med. Chem. Lett. XXXX, XXX, XXX−XXX